PAPER

Check for updates

Picogram-level detection of endotoxin in human saliva using ultrasensitive surface enhanced Raman scattering in lateral flow assay devices

Adewale Adehinmoye [a] Daewoo Han, [b] Pietro Strobbia [a] and Andrew J. Steckl [b]

The lateral flow assay (LFA) is the most popular rapid diagnostic tool due to its low cost, ease-of-use and fast response. However, conventional LFA design suffers from relatively low sensitivity and lack of quantification capability. In this study ultrasensitive and quantitative LFA device has been developed using surface-enhanced Raman scattering (SERS) detection to detect picogram level of *P. gingivalis* endotoxin, a major oral health biomarker, in human saliva. Silver coated gold nanostars (Ag@AuNS) with high SERS scattering efficiency were conjugated with Raman reporter (label) dye molecules. Saliva samples from multiple individuals were collected and pretreated to successfully remove components that interfere with endotoxin detection in saliva. The use of LFA cassettes leads to dramatic enhancement of LFA sensitivity and consistency by controlling the saliva flow rate (~29 seconds slower flow rate than the normal LFA strip) and assuring contact between membranes in the LFA. Significant LOD improvements were obtained using Ag@AuNS: 18 pg mL^{-1} and 0.3 ng mL^{-1} for SERS and colorimetric detection, respectively.

Introduction

The lateral flow assay (LFA) test is currently one of the most widely used rapid diagnostic tests (RDT), usually performed in point-of-care (POC) settings. While historically utilized for pregnancy, influenza and other assays, the COVID-19 pandemic greatly expanded the use of LFA tests worldwide.[1,2] Compared to lab-based quantitative methods of detection, such as polymerase chain reaction (PCR) and enzyme-linked immunosorbent assay (ELISA), LFA tests are much faster and cheaper and do not require technical operators. However, the output of LFAs is usually binary (yes/no) and its sensitivity is limited.[3] Raman spectroscopy (RS), a non-invasive and non-destructive technique that is especially helpful for examining a wide variety of molecules, is employed to improve the sensitivity and quantification of LFAs.[4,5] In specialized instances, surface-enhanced Raman spectroscopy (SERS), an improved variant of Raman spectroscopy, increases the signal from molecules close to specific metallic nanostructures by a factor of 10^6–10^8, resulting in single-molecule sensitivity.[6–8] SERS is being investigated to improve LFAs detection sensitivity and add quantification capabilities.[9–13] SERS employs metal nanoparticles (NPs) to amplify the Raman scattering of molecules on the metal NP surface, due to localized surface plasmon resonances (LSPRs).[14–16] SERS can be integrated into the operation of LFA devices, which already use NPs for visual detection, by adding Raman reporter molecules on the NPs and detecting Raman scattering signal from the LFA detection regions.[17,18] An additional advantage of this SERS+LFA is its highly multiplexing capabilities, which enables detection of multiple biomarkers during analysis.[13,17,19–21] The analytical performance of SERS+LFA depends on SERS signal from the NPs optically excited "hotspots" on the surface of NPs.[15,22–25] Conventional spherical NPs, typically gold and silver (AuNP, AgNP) provide limited hotspot generation.[22] However, silver-coated gold nanostars (Ag@AuNS) which have a branched structure can generate dense hotspots because of the nanogaps or nanotips having higher SERS scattering efficiency.[16,22,25,26]

Previously, we have reported on the use of LFAs for PoC detection of key biomarkers in several key physiological fluids (blood, sweat, urine, saliva).[27–31] Saliva is particularly attractive as a biofluid test medium because of its ready availability in sufficient volumes and the presence of biomarkers of viral, bacterial and other medical conditions.[29,30,32–34]

Lipopolysaccharide (LPS) is one of the molecular components of a Gram-negative bacteria that reside in the oral cavity and is an endotoxin that released when bacteria die.[35–38] Endotoxins trigger a significant immune response in hosts and, thus, are useful biomarkers helpful for the diagnosis of various bacterial infections. *Porphyromonas gingivalis* (PG) is a prominent Gram-negative pathogenic bacterium that causes severe periodontitis.[29,34,39,40] Periodontal disease caused by bacteria infection is characterized by a long-lasting inflammation, leading to gum disease and potentially tooth loss.[39,41,42] Hence,

aDepartment of Chemistry, University of Cincinnati, Cincinnati, OH 45221, USA
bDepartment of Electrical and Computer Engineering, University of Cincinnati, Cincinnati, OH 45221, USA
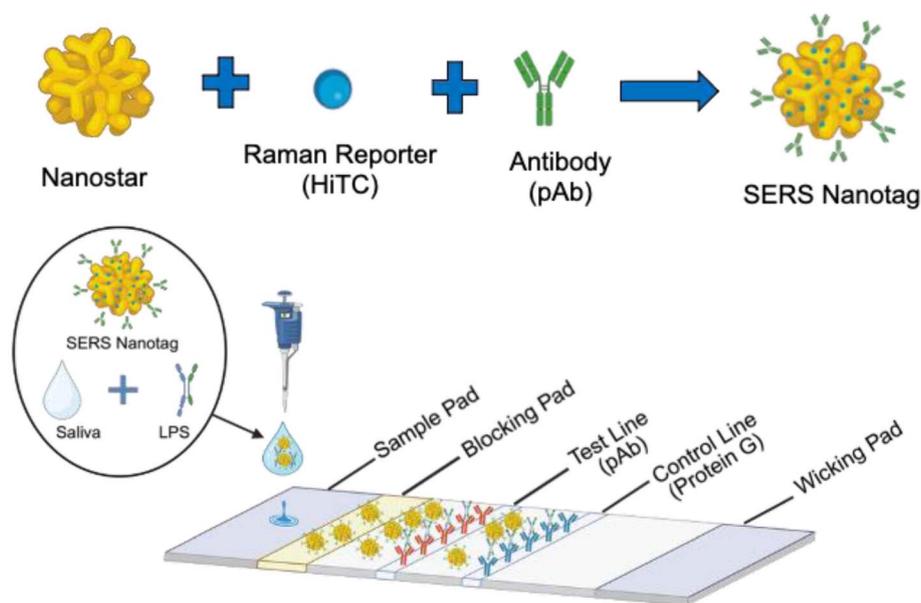
Paper

Fig. 1 Basic operation of the antibody sandwich LFA using the SERS Nanotag (created in BioRender).

the need to monitor the level of PG LPS is important for sound and healthy living. We have previously developed an LFA for the detection and quantification of PG LPS concentrations in human saliva using a sensitive sandwich-type immunoassay.[29] The colorimetric detection of PG LPS in human saliva achieved a limit of detection (LOD) of 46.5 ng mL^{-1} using Au NPs.[29] Improvements in LOD have been obtained using the SERS+LFA approach with several types of nanostars. Using silver-coated AuNS (Ag@AuNS), known to offer significantly enhanced SERS signal,[43] an LOD of < 10 ng mL^{-1} for PG LPS in buffer media was obtained.[17]

While the SERS+LFA approach has led to significant LOD improvement in buffer media, the ultimate application for oral health requires functioning in human saliva. Saliva is a complex medium, containing of a wide mixture of food particles, cell debris, and proteins that may alter the SERS+LFA function.[29,32] Herein, we demonstrate the first application of the SERS+LFA developed for PG LPS in *human saliva*. Specifically, we first investigate the cause of the observed loss-of-function ("instability") of NPs used in the SERS+LFA when applied to saliva, which is a significant divergence from the behavior of traditional/colorimetric LFA. Then, we demonstrate successful strategies to fix the observed instability. Finally, we report the use of the optimized SERS+LFA for the detection of biomarkers in saliva samples with pg mL^{-1}-level detection, covering the whole clinically relevant range of PG LPS concentrations for its final application.

The overall operation of the SERS+LFA device is illustrated in Fig. 1. The SERS Nanotag is formed by the conjugation of antibodies and Raman reporter (dye) molecules on the surface of the nanoparticles. After LFA strip fabrication, antibodies for target analytes (PG LPS) and protein G are printed for the test and control lines, as shown in Fig. S1. To obtain quantification of PG LPS in saliva, laser light at 785 nm wavelength is directed

on the test line where the flowing Nanotag is captured in presence of PG LPS. AuNPs and Ag@AuNS have been incubated overnight and thoroughly washed with 2.5 mM Tris–HCl PH 8.0 with 0.05% Tween-20. The UV-vis absorbance of both nanoparticle types was confirmed to be within the required range of 10 OD and 5 OD, before and after polyclonal antibody and tris–HCl buffer addition (Fig. S2a and b). TEM images confirm the preserved morphology of the washed AuNPs and Ag@AuNS (Fig. S2c and e). The test strips were inserted into standard LFA cassettes to replicate conventional usage and demonstrate POC applicability of the SERS+LFA analysis.

Experimental

Materials

The standard solution of 40 nm gold nanoparticles (10 OD) was obtained from Cytodiagnostics (Burlington, ON). 1 M hydrochloric acid, a 5.08 mM chloroauric acid solution (HAuCl4), ammonium hydroxide (NH$_4$OH), 1,1′,3,3,3′,3′-hexamethylindotricarbocyanine iodide (HiTC), Tween 20 (10% w/v), Triton™ X-100, L-ascorbic acid, *anti-P. gingivalis* LPS monoclonal and polyclonal antibodies, bovine serum albumin (BSA), and cellulose fiber pad (CFSP001700) were sourced from Sigma-Aldrich (St. Louis, MO). Silver nitrate (AgNO$_3$), sodium chloride, sodium phosphate tribasic dodecahydrate (Na$_3$PO$_4$·12H$_2$O, 98%, analysis grade), sucrose, Tris–HCl (1 M, pH 7.5 and 8), phosphate buffered saline (PBS, 10X, pH 7.4), trisodium citrate dihydrate, and 4-mercaptobenzoic acid were acquired from Fisher Scientific (Waltham, MA). Thiolated polyethylene glycol (HS-PEG, MW ≈ 5000 k) was obtained from Nanocs (New York, NY). All ultrapure *P. gingivalis* and *E. coli* LPS were obtained from InvivoGen (San Diego, CA). The glass fiber pad (8950) and nitrocellulose membrane (CN95) were supplied by Ahlstrom (Helsinki, Finland) and Sartorius (Goettingen, Germany),

respectively. The backing card measuring 60 (W) × 300 (L) mm was procured from Sartorius (Goettingen, Germany). All solutions were made using Millipore Synergy UV-R Ultrapure water (18.2 MΩ cm^{-1}). Artificial saliva was obtained from Pickering Laboratories (Mountain View, USA).

Silver coated gold nanostar synthesis

The John Turkevich method was used to synthesize approximately 12 nm gold seeds.[44] Ag@AuNS were synthesized by following previously established protocols.[43] To synthesize large nanostars, 493 μL of HAuCl$_4$ and 100 μL of gold seed solution were combined with 10 μL of 1 mM HCl while stirring vigorously. To first create the AuNS, AgNO$_3$ (10 μL) and L-ascorbic acid (10 μL) were added to the reaction vessel quickly, leading to a change in color from pale orange to deep blue. Then, to prepare Ag@AuNS, 50 μL of AgNO$_3$ and 10 μL of NH$_4$OH were introduced rapidly to the dark blue AuNP solution, and the mixture was stirred until the solution turned red-brown and the color stabilized. The Ag@AuNS particle solutions were kept at 4 °C until they were needed.

LFA strip fabrication process

The LFA strip comprises four components: a nitrocellulose membrane, a cellulose wicking pad, a cellulose sample pad, and a fiberglass blocking pad.

To begin, the nitrocellulose membrane (30 mm by 300 mm) and wicking pad (17 mm by 300 mm) are secured on an adhesive backing card and subsequently cut into 4.4-mm wide strips using the Biodot CM4000 automatic guillotine cutter (Biodot, Irvine, CA). Following that, protein G and *P. gingivalis* polyclonal antibody were printed as the control and test lines, respectively, utilizing the Biodot AD1500 printing system (Biodot, Irvine, CA). The optimal concentrations for both were determined to be 1 mg mL^{-1}, leading to stronger test and control line formations. After printing, the strips were incubated in an oven at 50 °C for 10 minutes and then stored in a light-protected nitrogen-purging environment to maintain their integrity.

The sample pads were precut to dimensions of 13 mm × 4.4 mm using a guillotine cutter. The blocking pads were prepared to dimension of 10 mm × 4.4 mm using a universal CO$_2$ laser system. Both pads were treated with various functional chemicals to perform key functions (*e.g.*, ensuring uniform flow, preventing non-specific binding) during the LFA test. The sample pads were soaked in a buffer solution consisting of 2.5 mL of Tris–HCl at 1 M with a pH of 8, 2.5 μL of 3 M NaCl solution, and 125 μL of Triton X-100, diluted in 50 mL of ultrapure water. The blocking pads were also immersed in a blocking buffer solution, formed by dissolving 250 mg of BSA, 500 mg of sucrose, 38.1 mg of Na$_3$PO$_4$ tribasic salt, and 12.5 μL of Tween-20 surfactant sequentially in 5 mL of ultrapure water. Both types of pads were soaked in their respective solutions for 40 min, then dried in an oven at 60 °C for 90 min and finally stored in a nitrogen-purging box overnight.

To complete the LFA fabrication, the treated sample and blocking pads were placed on the backing card, which had already been assembled with the nitrocellulose membrane and wicking pad before the LFA tests. For LFA tests, the fabricated LFA strip was placed inside the plastic cassette and the 90 μL of the sample solution was dispensed into the reservoir of the LFA cassette. The sample solution is comprised of 30 μL of functionalized nanoparticles solution, 10 μL of 3-M NaCl solution, 10 μL of saliva, 10 μL of PG LPS, and 30 μL of Tris–HCl (pH 8) buffer with 0.05% Tween-20. It was dispensed on the LFA devices after incubating for 40 min at room temperature.

Functionalization of nanoparticles with Raman reporter and antibody

A 1 mL of the nanomaterial solution (AuNP or Ag@AuNS, 10 OD) was mixed with 100 μL of 5 μM HiTC and the combination was incubated for 1 hour at room temperature. Following incubation, 11 μL of Tween-20 was introduced to the mixture. The samples were thoroughly vortexed and centrifuged at 3900 g for 10 min at 25 °C to separate the particles from the excess Raman reporter in the solution. The supernatant with excess Raman reporters was discarded, and the particles were re-dispersed in PBS 0.01× buffer. After successfully conjugating the nanomaterials with the Raman reporter, 5 μL of PG LPS polyclonal antibody (1 mg mL^{-1}) was added to 200 μL of nanomaterial solutions. Then, 195 μL of 2.5 mM Tris–HCl pH 8.0 with 0.05% Tween-20 surfactant was also incorporated. The combined solutions were incubated overnight in the refrigerator. After incubation, the solutions were centrifuged at 1300 g for 20 min, followed by removal of the supernatant and addition of fresh buffer solution composed of 2.5 mM Tris–HCl with pH 8.0 and 0.05% Tween-20. This washing cycle was performed 4 times. After the fourth washing cycle, the concentrations of nanomaterials were adjusted to 5 OD using a buffer solution.

Transmission electron microscopy

For TEM imaging, 10 μL of the nanomaterial solution was dispensed on the 300-mesh grid and allowed to dry overnight. A Talos F200i TEM with a field emission of 200 kV (Thermofisher) was used to acquire the images. This instrument was used at the Advanced Material Characterization Center (AMCC) at the University of Cincinnati.

UV-vis spectroscopy

The Synergy HTX multi-mode plate reader (BioTek, Winooski, VT) and Gen5 software (v3.10) collected absorbance spectra in a 96-well plate. 100 μL of sample solution containing AuNPs and Ag@AUNS in the presence of Raman reporter (HiTC) was dispensed inside the well plate. The measurement range was 300–900 nm, and blanks were subtracted from the spectrum in the native software.

Zeta potential measurement

The Zetasizer Pro (Malvern Panalytical, UK) was used to measure the charge on the surface of the material of interest. The 1 mL of sample solution is placed in a DTS1070 closed capillary electrophoresis cell that contains a gold-plated copper

electrode. For each sample, measurement was performed five times for 120 s each.

SERS measurements with Raman

SERS measurements were obtained using a custom benchtop Raman system, which included a Wasatch Photonics WP785 spectrometer, an OptoEngine 785 nm laser source (FC-D-785-300 mW), and a Raman fiber optic probe (Raman Probe by InPhotonics). The laser power was set to 74 mW during the measurements. The fiber optic probe was linked to a 2D (X–Y) motorized stage (Zaber) controlled by a LabVIEW software. This stage facilitated spectrum collection on the LFA. For the LFA operation targeting the specific analyte, spectra were obtained along the LFA strip through six parallel line-scans (15 points with a 1 mm step-size, covering both test and control line regions), with 0.5 mm spacing between lines. The line scans were averaged in the results presented. Each measurement had an integration time of 100 ms with 5 accumulations. Fig. S3 shows the Raman system used for all analysis and the illustration of the LFA strip measurement. On the LFA strip, point 4 is the control line and point 11 is the test line.

Image and data analysis

The LFA colorimetric output was processed using the NIH ImageJ software. The mean intensity of the LFA lines was measured using a fixed size for all measurements. The Raman data was processed using a MATLAB script (R2021b) (The Mathworks, Inc., Natick, MA). The SERS response was determined from the normalized peak of HiTC at 546 cm^{-1}. The data was plotted on IGOR Pro.

Results and discussion

Different volumes of saliva collected orally using a Pure•SAL™ (Oasis Diagnostics) saliva collector were used for analysis. Saliva was added to sample solutions with and without (SERS+LFA) HiTC. The analysis was performed using a single control line on LFA to evaluate the effect of saliva volume in immunoreactions on LFA. Fig. 2a shows images of the tests containing different volumes of saliva. For samples without HiTC, there was no visually observable interference up to at least 10 μL saliva volume (out of 90 μL total sample volume), whereas for samples with HiTC there was interference at all saliva volumes, including the lowest volume of 2 μL (∼2.2% of total sample volume). To quantify this behavior, LFA images were analyzed using ImageJ, as shown in Fig. 2b. The colorimetric image analysis of LFA strips for samples with and without HiTC indicates a similar trend of decreasing signal intensity with increasing saliva volume for both cases, but with more dramatic decrease to almost no-response for the HiTC-coated nanoparticles. Interestingly, for the LFA "control" strip with HiTC only (without saliva) analyte detection was observed.

To explore the cause of the observed behavior, the zeta potential of nanoparticles was measured in several conditions (Fig. 3): (i) increasing concentration (*i.e.* surface coating) of HiTC; (ii) addition of antibody molecules; (iii) in saliva. The zeta potential of pure AuNPs was −44.86 mV, monotonically decreasing with the addition of HiTC, reaching −36.4 mV with 5 μM HiTC (concentration used for SERS+LFA) and −31.5 mV with 20 μM HiTC. The addition of antibodies and saliva also had a similar decreasing effect on the zeta potential (Table. S1), with final SERS Nanotag combination (AuNP + HiTC 5 μM + pAb)
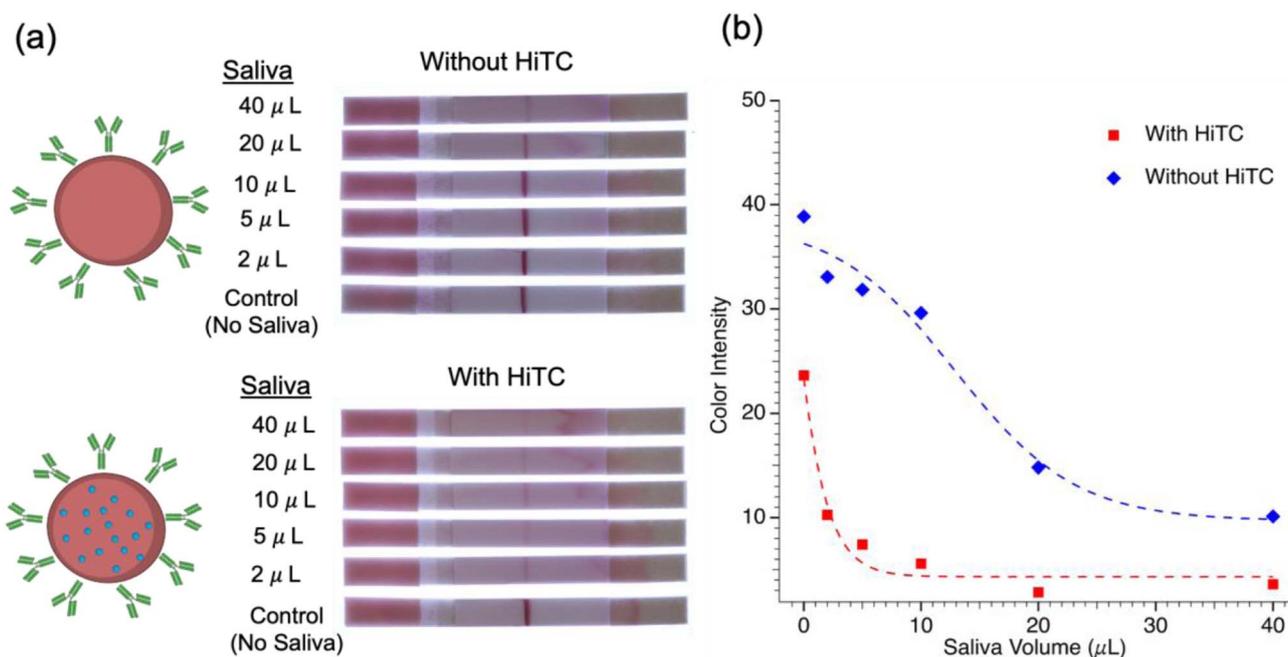

Fig. 2 LFA strip operation with and without HiTC for different saliva volumes: (a) photographs of LFA strips; (b) color intensity of the test lines (ImageJ).
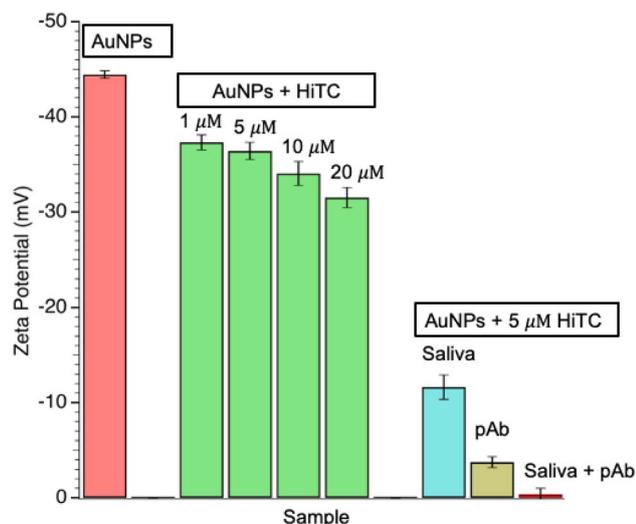
Fig. 3 Zeta potential for AuNPs under various conditions: Au NPs ("naked"), with several concentrations of HiTC Raman reporter (AuNPs + HITC); saliva, polyclonal antibody (pAb), saliva + pAb(AuNPs + 5 μM HITC).

reaching a zeta potential close to 0 mV in saliva. Specific zeta potential values are reported in the SI (Fig. S4). Nanoparticle charge is known to be a predictor of stability of suspension in solution, due to the tendency of these systems to aggregate in the absence of repulsive forces. The zeta potential results indicate that the effect of biofouling saliva compounded to the charge of HiTC cause suspension instability, which is likely responsible of the observed behavior of the SERS+LFA with saliva samples (Fig. 2).

One of the challenges in using saliva as the physiological fluid for the assay is segregating the biomarker of interest for investigation to prevent biochemical interferences.[29,45] Specifically, the amylase protein in saliva has been confirmed to be a major cause of saliva interference.[46]

Saliva is known to contain multiple proteins, including some with high abundance, such as amylase and mucin, which can interfere with the detection of proteins with lower abundance. Previously, mucin and amylase were separately tested against PG LPS.[29] It was observed that PG LPS was detectable in the presence of mucin, whereas amylase prevented the immuno-reactions on the LFA test strip. Hence, this indicates that the amylase protein causes interference during saliva LFA analysis. To remove amylase, starch is employed because it forms a crosslink with amylase.[29] This results in the depreciation of amylase, thereby improving the sensitivity of PG LPS in human saliva.

This low-cost potato starch reaction was utilized to sequester amylase in the sample. In addition, a double filtration step was used to remove unwanted debris found in saliva. 400 μL of saliva is pipetted into a syringe with a titan cellulose syringe filter with pore size 0.20 μm, then 200 mg of potato starch is placed into the syringe (Fig. 4a). Then the mixture of potato starch and saliva is gently filtrated. A comparison between Pure•SAL™ saliva collectors containing single and double filters established that the double filter case produces visually clearer control and test lines and a SERS signal enhancement of ~2.5×, as seen in Fig. 4b. Another comparison was performed between the as-collected saliva (no pretreatment) and pre-treated saliva (with pretreatment), as shown in Fig. 4c. Both are collected using double filter Pure•SAL™ saliva collectors. The SERS intensity for the pretreated saliva produced a stronger signal for both the test and control lines. These results
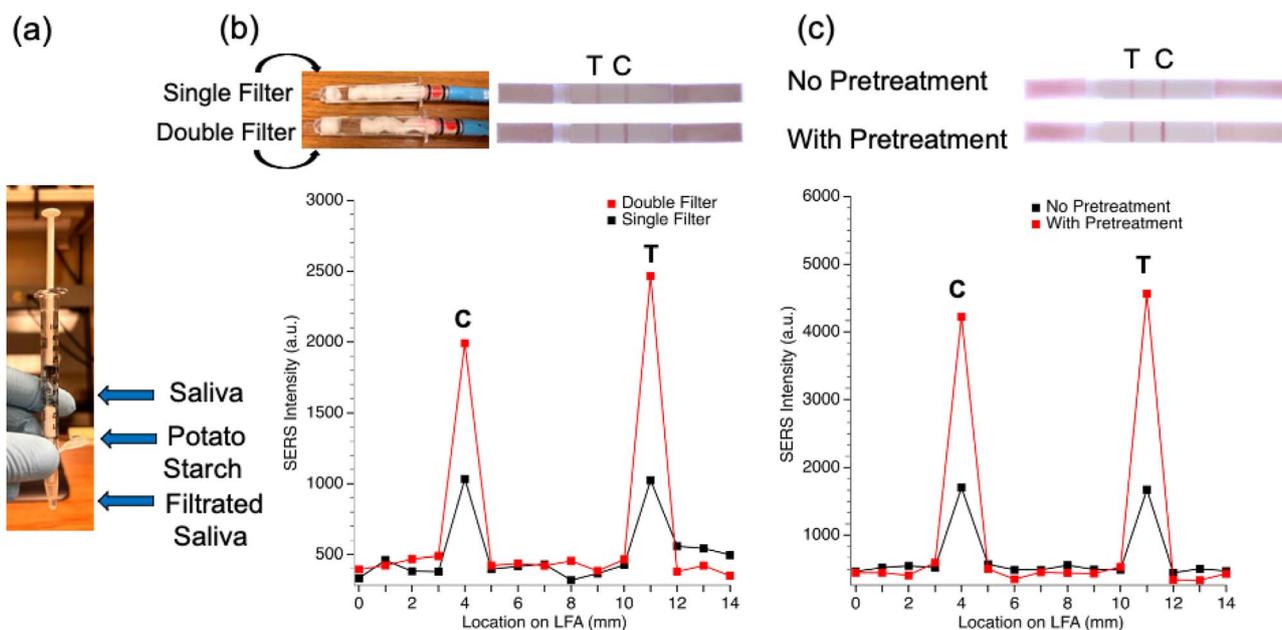

Fig. 4 Saliva pretreatment process: (a) use of saliva filter and starch in syringe; (b) SERS signal for saliva samples with single and double filter treatment; (c) SERS signal comparison using double filter with and without pretreatment.
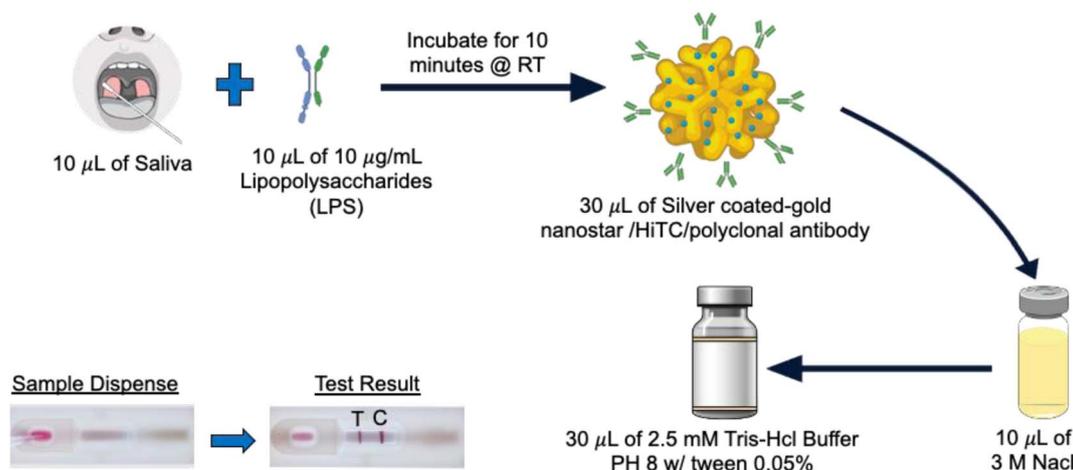
Fig. 5 SERS-LFA sample preparation process for detection of PG LPS in human saliva.
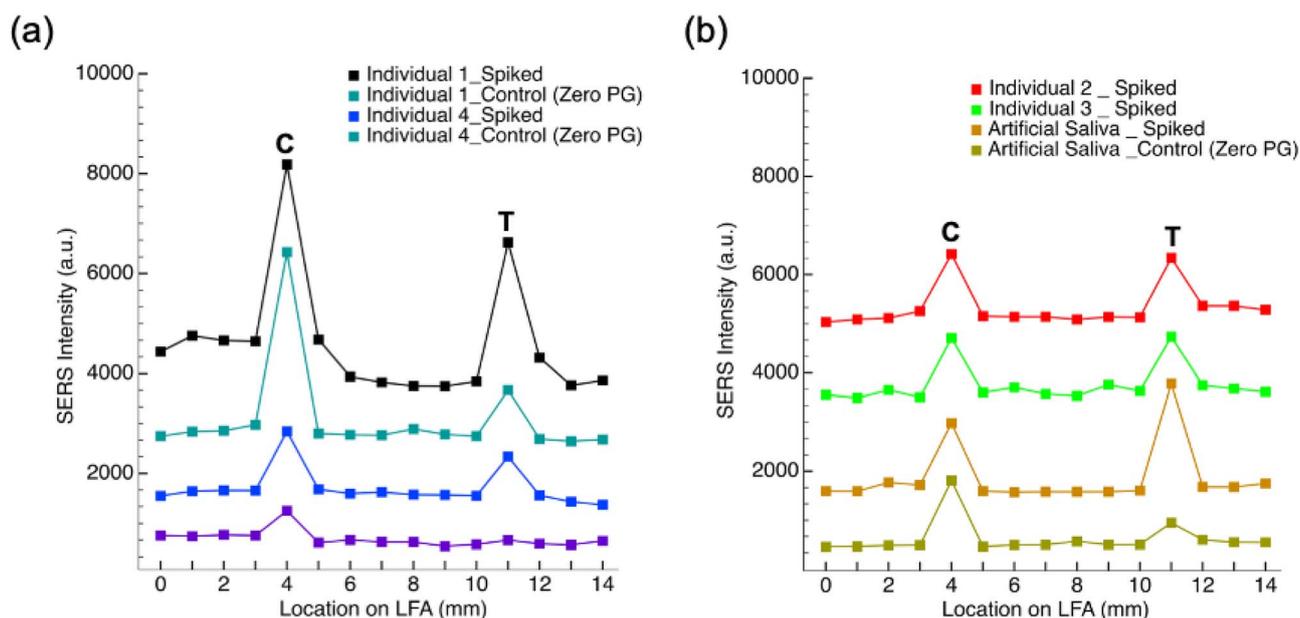

Fig. 6 Detection of PG LPS (10 µg mL^{-1}) spiked in saliva from several individuals – photographs of individual LFA cassette kits and corresponding SERS-LFA results: (a) individual 1 – LPS present in non-spiked saliva, individual 2 – LPS not present in non-spiked saliva; (b) spiked saliva from individuals 2 and 3 presents very similar response, LPS detection in spiked and unspiked artificial saliva.

demonstrate that the use of the starch reaction combined with double filtration can stabilize the SERS Nanotags used for SERS+LFA (*i.e.*, AuNP coated with 5 µM HiTC), enabling the use of this powerful assay in real samples. The SERS spectra in Fig. S5 indicate (highlighted) the main detection peak of HiTC at 546 cm^{-1}. The reproducibility of SERS in this LFA analysis using pretreated saliva can be seen in Fig. S6. Interestingly, the zeta potential after saliva pretreatment increased from close to zero mV to approximately 14 mV.

To prepare a saliva sample solution for SERS+LFA measurements, first 10 µL of pretreated saliva is dispensed into a µcentrifuge tube. Next, 10 µL of 10 µg mL^{-1} PG^{-1} LPS is added, and the mixture is allowed to sit for 10 minutes at room

temperature (RT). Then, 30 µL of SERS nanotag solution was added, followed by 10 µL of 3 M NaCl, 30 µL of 2.5 mM Tris–HCl buffer with 0.05% Tween-20. This results in a total sample solution of 90 µL. There is no need to incubate the total sample mixture for long time period, as incubation has little or no effect on the SERS signal, as seen in Fig. S7. Finally, the saliva sample solution is dispensed onto the reservoir of LFA cassettes to simulate eventual POC use in the field. The overall process is illustrated in Fig. 5. The LFA operation was first tested with buffer solution samples. As seen in Fig. S8, the Ag@AuNS yields a higher SERS intensity in buffer than AuNPs, confirming the stronger SERS scattering properties of Ag@AuNS that had been established previously.
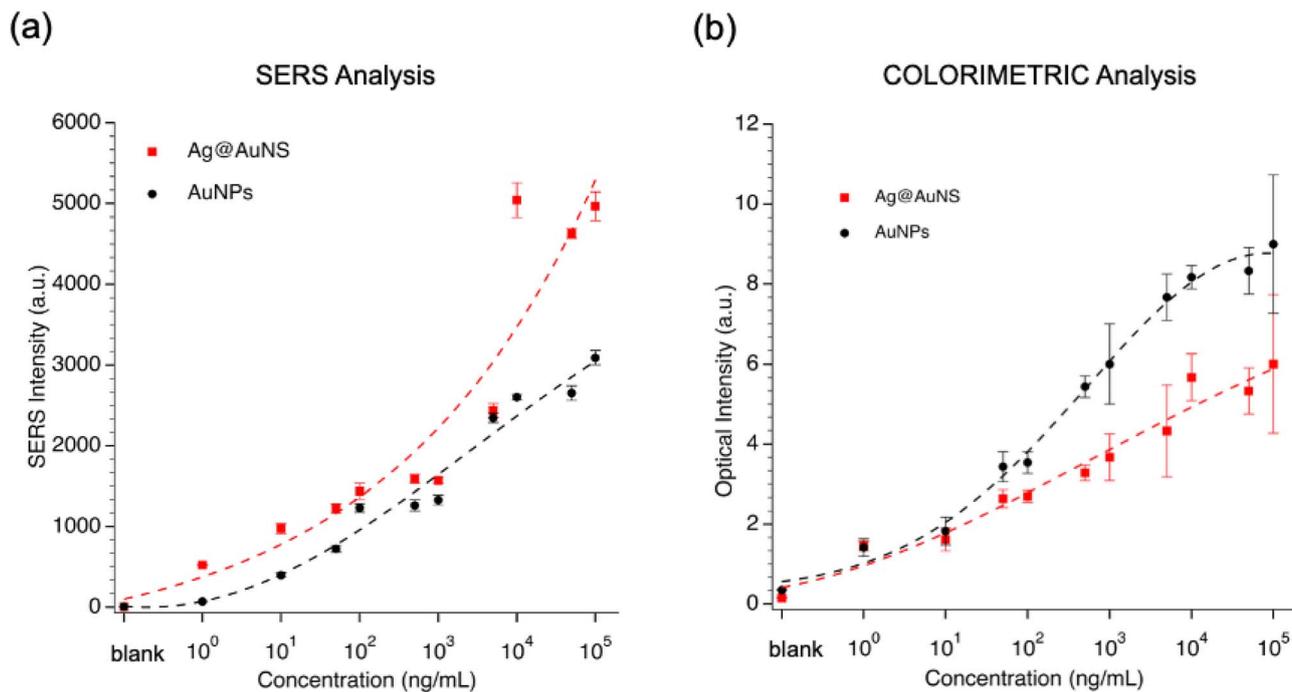
(a)

(b)

Fig. 7 SERS (a) and colorimetric (b) analysis of saliva with LPS mixtures (1–100,000 ng mL^{-1}), using both AuNPs and Ag@AuNS. Blank − negative control (zero LPS concentration). Dashed lines are aids for trend visualization ($n = 3$).

To determine broader applicability of this method, different saliva samples from several individuals were collected and evaluated. All saliva samples were first pretreated and then spiked with 10 μg mL^{-1} PG^{-1} LPS. Contrasting test results from individuals 1 and 4 are shown in Fig. 6a: SERS signal of the test cassettes for each case. For individual 4, the test line for the control case (non-spiked) was not formed, indicating no (or negligible) presence of native LPS in collected saliva, while the spiked case presented a small but clear signal on the test line, as seen in Fig. S9a. In contrast, the control case for *individual* 1 presented a noticeable peak on the test line, indicating the possible presence of measurable native LPS, while for the spiked case a large signal is observed on the test line. The test results for individuals 2 and 3 (Fig. 6b) are similar to individual 4, with similar spiked and control test lines indicating a low presence of native LPS. Clearly the assay can distinguish between "normal" results (low native LPS) and "oral alert" (high native LPS) cases. Artificial saliva was also tested for SERS+LFA tests to determine its suitability as a substitute for human saliva. The spiked artificial saliva produced a large LPS signal, presumably because of the absence of other competing proteins, indicating that it might not be a representative substitute (Fig. S9b). Interestingly, the control line of individual 1 shows stronger intensity than other individuals. Although the saliva was pretreated to inhibit amylase effects to improve immunoreactions of saliva samples, possibly there are other components or conditions that may still affect the immunoreactions on LFA. The reproducibility of this study is shown in bar plot representation in Fig. S10. Further investigations will be carried out into this aspect in the future.

To evaluate the performance of SERS+LFA on saliva sample, calibration curves were obtained comparing SERS and colorimetry modalities using different type of nanoparticles. Very wide range of LPS concentrations, from 0–100,000 ng mL^{-1} were tested with human saliva. Both AuNPs and Ag@AuNS were evaluated in order to have a comparison between the two nanomaterials and the two methods of quantification, SERS and colorimetric (using ImageJ) analysis. LFA tests were performed in triplicates for AuNPs and Ag@AuNS (Fig. S11a and b, respectively). The SERS and colorimetric signals from the test lines of both AuNPs and Ag@AuNS were plotted against the LPS concentration, as shown in Fig. 7. As expected, Ag@AuNS produce a stronger SERS signal than AuNPs, while the AuNPs provide a better image analysis data than Ag@AuNS, largely due to the colorimetric brightness of the AuNPs.

The LOD concentration for PG LPS in saliva calculated[47] from the data in Fig. 7 is summarized in Table 1. Using Ag@AuNS results in a superior LOD compared to AuNPs for both SERS and colorimetric analysis. Ag@AuNS has a SERS LOD of 18 pg mL^{-1}, which is ~4× more sensitive than SERS AuNPs. The LOD for colorimetric analysis is not as sensitive as SERS analysis and is ~15× higher than the best SERS result.

Table 1 LOD concentration for PG LPS in human saliva − comparison of SERS and colorimetric analysis as method of quantification using AuNPs and Ag@AuNS

	AuNPs		Ag@AuNS	
	Colorimetric	SERS	Colorimetric	SERS
LOD	0.384 ng mL^{-1}	0.080 ng mL^{-1}	0.307 ng mL^{-1}	0.018 ng mL^{-1}

Summary and conclusions

In summary, picogram-level detection of *P. gingivalis* endotoxin (major oral health biomarker) in human saliva was obtained using ultrasensitive surface enhanced Raman scattering (SERS) detection. Using SERS detection w. NanoTags [a combination of Ag-coated Au nanostars, HiTC (a Raman reporter dye) and an antibody] a dynamic range of 5^+ orders of amplitude has been achieved. The LOD for SERS detection using Ag@AuNS is 18 pg mL^{-1}, which is ~4× more sensitive than SERS AuNP analysis. By comparison the LOD for colorimetric analysis is ~15× higher than the best SERS result. Because of the very low LOD and wide enough dynamic range, the LFA+SERS platform has the potential to lead to a paradigm shift in home-test moving from yes/no answers to quantification of biomarkers useful in many POC applications.

When obtaining saliva samples from healthy volunteers, there is a possibility that the saliva contains small amounts of PG LPS. However, it is very challenging to obtain the accurate concentration of PG LPS for healthy individuals. There is no commercially available assay or approach to measure the PG LPS concentration. To resolve this issue to the best of our ability, we evaluated artificial saliva and compared it with human saliva results, which presented even higher intensity than unspiked human saliva samples. In the current approach an antibody has been used for capturing the target PG LPS in the SERS+LFA platform. In the future, we plan to explore more flexible and affordable aptamers in order to enhance the assay sensitivity and also expand the linear dynamic range. The aptamer-based SERS+LFA platform will expand the range of applications related to many other diseases.

Conflicts of interest

The authors declare that there are no conflict of interests to disclose.

Data availability

The data supporting this article, such as LFA fabrication process, SERS setup & measured spectra, zeta potential, effects if double filter and incubation time, and LFA results using different human saliva, have been included as part of the supplementary information (SI). Supplementary information is available. See DOI: https://doi.org/10.1039/d5ra04515k.

Acknowledgements

References

1 L. Khelifa, Y. Hu, N. Jiang and A. K. Yetisen, *Lab Chip*, 2022, **22**, 2451–2475.

2 Y. Liu, L. Zhan, Z. Qin, J. Sackrison and J. C. Bischof, *ACS Nano*, 2021, **15**, 3593–3611.

3 J. Budd, B. S. Miller, N. E. Weckman, D. Cherkaoui, D. Huang, A. T. Decruz, N. Fongwen, G.-R. Han, M. Broto, C. S. Estcourt, J. Gibbs, D. Pillay, P. Sonnenberg, R. Meurant, M. R. Thomas, N. Keegan, M. M. Stevens, E. Nastouli, E. J. Topol, A. M. Johnson, M. Shahmanesh, A. Ozcan, J. J. Collins, M. Fernandez Suarez, B. Rodriguez, R. W. Peeling and R. A. McKendry, *Nat. Rev. Bioeng.*, 2023, **1**, 13–31.

4 E. Smith and G. Dent, in *Modern Raman Spectroscopy: A Practical Approach*, John Wiley & Sons, Ltd, 2019, ch. 2, pp. 21–75.

5 E. Smith and G. Dent, in *Modern Raman Spectroscopy: A Practical Approach*, John Wiley & Sons, Ltd, 2019, ch. 2, pp. 77–99.

6 M. Moskovits, *J. Raman Spectrosc.*, 2005, **36**, 485–496.

7 D. L. Jeanmaire and R. P. V. Duyne, *J. Electroanal. Chem. Interfacial Electrochem.*, 1977, **84**, 1–20.

8 R. Pilot, R. Signorini, C. Durante, L. Orian, M. Bhamidipati and L. Fabris, *Biosensors*, 2019, **9**(2), 57, DOI: 10.3390/bios9020057.

9 X. Cao, Q. Song, Y. Sun, Y. Mao, W. Lu and L. Li, *Nanotechnology*, 2021, **32**, 445101.

10 S. Srivastav, A. Dankov, M. Adanalic, R. Grzeschik, V. Tran, S. Pagel-Wieder, F. Gessler, I. Spreitzer, T. Scholz, B. Schnierle, O. E. Anastasiou, U. Dittmer and S. Schlücker, *Anal. Chem.*, 2021, **93**, 12391–12399.

11 S. Yan, C. Liu, S. Fang, J. Ma, J. Qiu, D. Xu, L. Li, J. Yu, D. Li and Q. Liu, *Anal. Bioanal. Chem.*, 2020, **412**, 7881–7890.

12 R. Frimpong, W. Jang, J.-H. Kim and J. Driskell, *Talanta*, 2021, **223**, 121739.

13 W. A. Hassanain, J. Spoors, C. L. Johnson, K. Faulds, N. Keegan and D. Graham, *Analyst*, 2021, **146**, 4495–4505.

14 J. Li, J. Xu, Y. Pan, Y. Zhu, Y. Wang, S. Chen and X. Wei, *Food Sci. Hum. Wellness*, 2023, **12**, 912–919.

15 L. Blanco-Covián, V. Montes-García, A. Girard, M. T. Fernández-Abedul, J. Pérez-Juste, I. Pastoriza-Santos, K. Faulds, D. Graham and M. C. Blanco-López, *Nanoscale*, 2017, **9**, 2051–2058.

16 D. Vang and P. Strobbia, *Appl. Spectrosc.*, 2023, **77**, 270–280.

17 L. N. Kissell, D. Han, D. Vang, A. W. R. Cikanek, A. J. Steckl and P. Strobbia, *Sens. Diagn.*, 2024, **3**, 839–849.

18 H. T. Ngo, E. Freedman, R. A. Odion, P. Strobbia, A. S. De Silva Indrasekara, P. Vohra, S. M. Taylor and T. Vo-Dinh, *Sci. Rep.*, 2018, **8**, 4075.

19 X. Wang, N. Choi, Z. Cheng, J. Ko, L. Chen and J. Choo, *Anal. Chem.*, 2017, **89**, 1163–1169.

20 C. Wang, C. Wang, J. Li, Z. Tu, B. Gu and S. Wang, *Biosens. Bioelectron.*, 2022, **214**, 114525.

21 Z. Wu, *Food Anal. Methods*, 2019, **12**, 1086–1091.

22 Y. Wu, Q. Yang, J. Chen, L. Bi, Z. Zhang, N. Zhou, A. Ostovan, M. Arabi, L. Chen and J. Choo, *ACS Appl. Nano Mater.*, 2024, **7**, 27134–27141.

23 N. H. Kim, S. J. Lee and M. Moskovits, *Adv. Mater.*, 2011, **23**, 4152–4156.

24 C. G. Khoury and T. Vo-Dinh, *J. Phys. Chem. C*, 2008, **112**, 18849–18859.

25 L.-K. Lin and L. A. Stanciu, *Sens. Actuators, B*, 2018, **276**, 222–229.

26 D. Han, D. Vang, A. Adehinmoye, L. Kissell, P. Strobbia, and A. J. Steckl, 2024, pp. 320–323, DOI: **10.31438/trf.hh2024.86**.

27 S. Dalirirad and A. J. Steckl, *Sens. Actuators, B*, 2019, **283**, 79–86.

28 S. Dalirirad and A. J. Steckl, *Anal. Biochem.*, 2020, **596**, 113637.

29 D. Han, S. Xie and A. J. Steckl, *Sens. Diagn.*, 2023, **2**, 1460–1468.

30 S. Dalirirad, D. Han and A. J. Steckl, *ACS Omega*, 2020, **5**, 26860–26868.

31 A. J. Steckl and P. Ray, *ACS Sens.*, 2018, **3**, 2025–2044.

32 T. W. Pittman, D. B. Decsi, C. Punyadeera and C. S. Henry, *Theranostics*, 2023, **13**, 1091–1108.

33 E. B. Aydın, M. Aydın and M. K. Sezgintürk, in *Advances in Clinical Chemistry*, ed. G. S. Makowski, Elsevier, 2023, vol. 113, pp. 1–41.

34 S. Zaric, A. Strachan, Y. Kurushima, A. Dong, C. McIlwaine, Z. Harrington, L. Nibali, A. Foey and M. Ide, *Front. Oral Health*, 2022, **3**, 1–9.

35 S. H. Rhee, *Intest. Res.*, 2014, **12**, 90–95.

36 B. S. Park and J.-O. Lee, *Exp. Mol. Med.*, 2013, **45**, e66.

37 P.-L. Wang and K. Ohura, *Crit. Rev. Oral Biol. Med.*, 2002, **13**, 132–142.

38 S. Xie, C. Haught, C. Tansky, M. Klukowska, P. hu, D. Ramsey, B. Circello, T. Huggins and D. White, *Am. J. Dent.*, 2018, **31**, 215–224.

39 J. Mysak, S. Podzimek, P. Sommerova, Y. Lyuya-Mi, J. Bartova, T. Janatova, J. Prochazkova and J. Duskova, *J. Immunol. Res.*, 2014, **2014**, 476068.

40 S. R. Lyons, A. L. Griffen and E. J. Leys, *J. Clin. Microbiol.*, 2000, **38**, 2362–2365.

41 W. He, M. You, W. Wan, F. Xu, F. Li and A. Li, *Trends Biotechnol.*, 2018, **36**, 1127–1144.

42 C.-K. Chen, Y.-T. Wu and Y.-C. Chang, *Alzheimer's Res. Ther.*, 2017, **9**, 56.

43 A. M. Fales, H. Yuan and T. Vo-Dinh, *J. Phys. Chem. C*, 2014, **118**, 3708–3715.

44 J. Turkevich, P. C. Stevenson and J. Hillier, *Discuss. Faraday Soc.*, 1951, **11**, 55.

45 A. Sen, H. Poulsen, S. Sondhauss and J. M. Hodgkiss, *ACS Sens.*, 2023, **8**, 1841–1849.

46 O. Deutsch, Y. Fleissig, B. Zaks, G. Krief, D. J. Aframian and A. Palmon, *Electrophoresis*, 2008, **29**, 4150–4157.

47 D. Armbruster and T. Pry, *Clin. Biochem. Rev.*, 2008, **29**(Suppl 1), S49–S52.